

Convolutional Neural Networks with Transfer Learning for Pneumonia Detection

Orlando Iparraguirre-Villanueva¹, Victor Guevara-Ponce², Ofelia Roque Paredes³, Fernando Sierra-Liñan⁴,
Joselyn Zapata-Paulini⁵, Michael Cabanillas-Carbonell⁶

Facultad de Ingeniería y Arquitectura, Universidad Autónoma del Perú, Lima, Perú¹

Escuela de Posgrado, Universidad Ricardo Palma, Lima, Perú^{2,3}

Facultad de Ingeniería, Universidad Privada del Norte, Lima, Perú⁴

Escuela de Posgrado, Universidad Continental, Lima, Perú⁵

Escuela Técnica Superior de Ingenieros de Telecomunicación, Universidad Politécnica de Madrid⁶

Vicerrectorado de Investigación, Universidad Norbert Wiener, Lima, Perú⁶

Abstract—Pneumonia is a type of acute respiratory infection caused by microbes, and viruses that affect the lungs. Pneumonia is the leading cause of infant mortality in the world, accounting for 81% of deaths in children under five years of age. There are approximately 1.2 million cases of pneumonia in children under five years of age and 180 000 died in 2016. Early detection of pneumonia can help reduce mortality rates. Therefore, this paper presents four convolutional neural network (CNN) models to detect pneumonia from chest X-ray images. CNNs were trained to classify X-ray images into two types: normal and pneumonia, using several convolutional layers. The four models used in this work are pre-trained: VGG16, VGG19, ResNet50, and InceptionV3. The measures that were used for the evaluation of the results are Accuracy, recall, and F1-Score. The models were trained and validated with the dataset. The results showed that the InceptionV3 model achieved the best performance with 72.9% accuracy, recall 93.7%, and F1-Score 82%. This indicates that CNN models are suitable for detecting pneumonia with high accuracy.

Keywords—Neural networks; transfer learning; pneumonia; detection; Convolutional

I. INTRODUCTION

Pneumonia is a type of acute respiratory infection caused by bacteria, viruses, or fungi that affects the lungs. Pneumonia is the leading cause of child mortality worldwide, with pneumonia killing an estimated 920136 children under five years of age in 2015, accounting for 15% of all deaths in children under five years of age worldwide [1]. Pneumonia is more prevalent in underdeveloped countries, where the lack of basic conditions is notorious, pollution worsens the situation and, at the same time, medical resources are increasingly scarce [2]. Therefore, early diagnosis and treatment play a very important role in preventing the disease from becoming fatal. Chest radiographs (X-rays) are most often used for the diagnosis of pneumonia. However, X-rays are prone to subjective variability [3][4]. Therefore, this paper presents four CNN models to detect pneumonia from chest X-ray images, which can be used by medical centers to detect pneumonia in their patients. The four deep CNN models were trained to classify the X-ray images into two types: normal and pneumonia.

The CNN-based transfer learning (TL) models used for this research work are: VGG16, VGG19, ResNet50, and InceptionV3, these models have been trained with the ImageNet database, a database with millions of images, and have obtained very satisfactory results, considered as successful. However, for this work, we used the Kaggle dataset, which is a less extensive dataset, basically due to computational resources. The four classification models were developed using CNNs for the purpose of detecting pneumonia from chest X-ray images. It is important to note that none of the four models used in this work have the same number of convolutional layers, so there is no direct relationship with the accuracy of the model [5]. Therefore, each of the models delivers different results with respect to accuracy. Each of the models follows its training architecture. To obtain the best accuracy in each model, at first, it is trained with a certain amount of convolutional combinations, dense layers, dropout, and other optimizers evaluating each model after each iteration, later, the complexity was increased to obtain a better model accuracy. The aim of this work is to classify and detect pneumonia from chest X-ray images, using CNNs with TL. If the model manages to achieve high accuracy, but with low recall values, it is considered an unreliable, ineffective, or even unsafe performance, since high false negative values represent a higher number of cases where the model predicts an output as normal, but in reality, the output is not normal. Therefore, to avoid this, we consider only the models with the highest recall and accuracy values [6] [7]. This is why, in the case of medical image processing, retrieval is preferred over other performance evaluation parameters.

This paper is organized as follows: Section 1 provides an introduction to the subject, addressing the problems, importance, purpose, and objective for undertaking this work. Section 2 explores the main works related so far. Section 3 describes the work methodology, the architectures of the models to be trained, the process diagram, and the data set to be trained. Section 4 presents the results obtained by the four CNN models and discusses the results. Finally, Section 5 provides the conclusions of the work.

II. RELATED WORK

Academic researchers and scientists in the medical sciences have published research papers addressing the problem of pneumonia detection with neural networks.

The authors in [5] presented a CNN model to detect pneumonia with high accuracy from chest images. The experiment worked with chest X-ray images, achieving an accuracy of 89.67%. Similarly, in [8][9] they developed work to automatically detect bacterial pneumonia, through the TL, for which they used 5247 chest X-ray images. Classifying in three groups: normal, bacterial, and viral pneumonia, obtaining results in classification accuracy of 98%, 95%, and 93%, respectively. Similarly, in [10] they developed four models: CNN, VGG16, VGG19, and InceptionV3, where they used TL techniques with CNN. They used 9992 normal chest radiographs and 2972 pneumonia. The results were tested with 854 pneumonia and 849 normal chest images, obtaining an accuracy higher than 97% in all four models. As well as, in [11] applied an automated TL approach with CNN using four pre-trained models (VGG19, DenseNet121, Xception, and ResNet50), to identify pneumonia. the performance of the four models provided an accuracy higher than 83.0%. Also, in [12] they trained different CNNs to classify X-ray images into two types, normal and pneumonia. As well as, in [13] they proposed a learning framework combining residual thinking and convolution to diagnose childhood pneumonia.

CNNs have the function of automatically extracting features. Currently, it is the area of choice for disease diagnosis related to radiographic image analysis, the purpose of which is to aid in the early detection of symptoms and risk factors of the Covid-19 virus. Also, [14] explored the effectiveness of AI to quickly and accurately identify COVID-19 from a set of images with different deep learning (DL) models and adjust them to achieve better detection accuracy of the best algorithms. Also, in [15] they evaluated the performance of CNN architectures for X-ray image classification, concluding that the procedure called TL produces the best results for the detection of various anomalies. Similarly, in [16] they proposed a DL technique based on object detection, CNN, and TL, combined with the pre-trained VGG19 model. For this, they used 1583 healthy samples and 5273 with pneumonia. The proposed model achieved an accuracy of over 99%.

III. METHODOLOGY

Convolution is the main element in the construction of a CNN. The convolution is composed of several layers of convolutional filters, to which activation functions and optimizers are added to achieve a better result. The work involves a series of steps, starting with the import of the dataset from Kaggle, and then the processing of the dataset is performed. Next, the dataset was trained with the following models: VGG16, VGG19, ResNet50, and Inception-v3 for classification. A total of 5216 chest X-ray images with Pneumonia were used for training and 624 for validation. The following sections describe the above steps in more detail. The phases of this work are shown in Fig. 1.

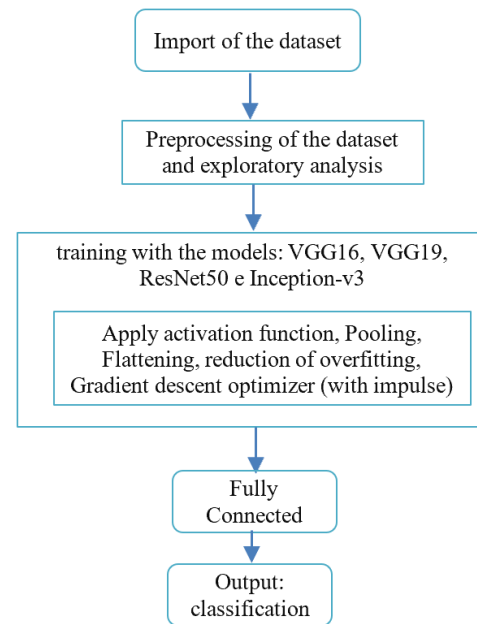


Fig. 1. Diagram of the Process that Follows the Work.

- Dataset Processing

For preprocessing, a total of 5840 images were used, divided into 5216 chest X-ray images for training and 624 for experimental validation. At this stage, we assigned the parameters and standardized the channel numbers, image dimensions, Batch size, validation size, regulation, and early stopping techniques, and applied the data for training and validation as shown in Fig. 2.

- Training with the Models

The images are classified into two types: normal and pneumonia, as shown in Fig. 3. In addition, fine-tuning is applied to match the outputs to the classes according to the problem. This consists of four densely connected layers; the first and second are assigned 4096 neurons respectively, the third is reduced to 1000 neurons, and finally, two neurons are used for the output, one for each class. Then the function to generate the model is applied, and with that, the training is started by defining the number of epochs, the batch size, the number of images to train, the number of test images, and the validation steps.

```
# Training
train_image_cogenerator = image_generator.flow_from_directory(
    train_path,
    target_size=image_shape[:2],
    color_mode='rgb',
    batch_size=batch_size,
    class_mode='categorical')

# Test
test_image_cogenerator = image_generator.flow_from_directory(
    test_path,
    target_size=image_shape[:2],
    color_mode='rgb',
    batch_size=batch_size,
    class_mode='categorical')
```

Fig. 2. Training and Test Code.

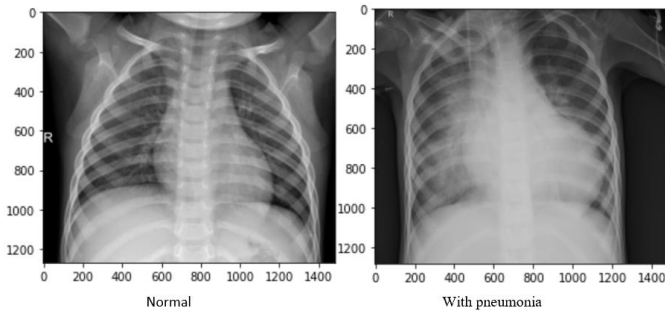


Fig. 3. Chest X-Ray Images Include Two Types of Images: Normal and with Pneumonia.

A. CNN Architecture

CNN is a type of multilayer artificial neural network. As shown in Fig. 4, it is composed of four convolutional layers and among other reduction layers, these are assigned alternately, and at the end, total connection layers are added, similar to a multilayer perceptron network. In the following, each of the layers is discussed.

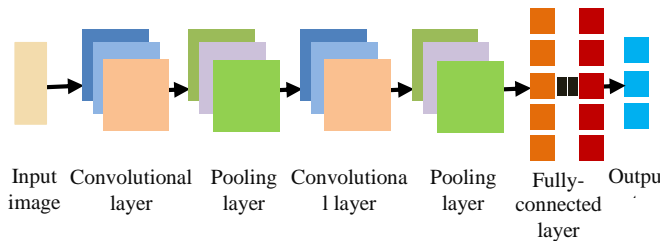


Fig. 4. CNN Architecture.

B. Convolutional Layer

The convolutional layer is in charge of processing the output of the neurons that are connected in the local input areas, calculating the product to be scaled between their weights. One of the functions of this layer is to reduce the dimensions of the images, facilitating their processing. However, this leads to the loss of some information, but the integral part of the image features is preserved since it is retained by the detector [17]. Also, in this layer filters, and attribute detectors were applied to the input matrix. Then a clustering process is applied to obtain our first convolutional layer.

C. Activation Functions

The activation function (AF) is the one that returns an output that is generated by the neuron given an input. Each of the layers that make up a neural network has an AF that allows prediction. The AF is divided into two types: linear and nonlinear. The linear function allows the input data to be equal to the output data, it is also applied when linear regression is required as output. Meanwhile, the nonlinear function is applied when you want to classify or when you have categorical outputs.

D. Pooling Layer

This layer is applied between the two convolution layers, as input, it receives the feature map formed at the output of the convolution layer; its main function is to reduce the size of the

images while preserving their most resolving features [18]. Finally, in the output of each Pooling layer, the same number of features is obtained as in the output, but considerably compressed [16].

The most commonly used clustering techniques with the different models are Max Pooling and Average Pooling. Also, max Pooling is used to create a feature map with reduced sampling. Average Pooling is used to calculate the average value of the filter size. The application of these two pooling techniques provides the ability to learn invariant features and also acts as a regularizer to reduce the overfitting problem. In addition, they significantly reduce the computational cost and training time of the networks, which are important criteria to consider.

E. Fully Connected Layer

This layer allows the feature maps generated from the neural network to be processed in a very facial way. Next, the image to be trained (input) passes through the convolution and clustering layer then enters the fully connected (FC) layer. In this way, the input image continues forward by calculating the weights. An FC neural network is composed of a set of FC layers and, connects to each neuron in a layer. The FC layer also functions as a classifier in the CNN. This layer has a behavior similar to a traditional network. For this case study, the FC layer is implemented through a convolutional operation. The FC layer is FC to the previous layer and, the convolution layer is used to replace the FC layer. Usually, a 1x1 convolution kernel is used. This type of CNN does not include an FC layer; thus, it can be converted into a full convolution of a neural network [19]. In Fig. 2, the first two layers are used to manage the features, while the last two layers are FC, and are used for classification.

F. Reducing Overfitting

The dropout technique was applied to reduce the overfitting in the VGG16, VGG19, and ResNet50 models. Dropout is a regulation technique based on the elimination of neurons in the neural network layers that are applied based on the probability given by the distribution [20]. The main objective of this technique is to mitigate the possible occurrence of phenomena known as overfitting. This phenomenon is very characteristic of neural networks and occurs in most training. There are multiple ways to reduce overfitting. Increasing the volume of data is one way to reduce overfitting, however, this leads to an increase in computational resources and training time.

G. Transfer Learning

With new advances in CNNs, the margins of error in image classification have been reduced. Models such as ResNet and DenseNet were developed to improve image classification, achieving exceptional performance in large-scale visual recognition. In recent years, TL has been used very successfully in different fields, such as manufacturing processes, medicine, and baggage screening, among others [21][8]. This has allowed eliminating the requirement of large amounts of data for training, it also allows reducing the training time, hence less computational resources. Fig. 5 shows the model from large volumes of data, and how it can be used for smaller data.

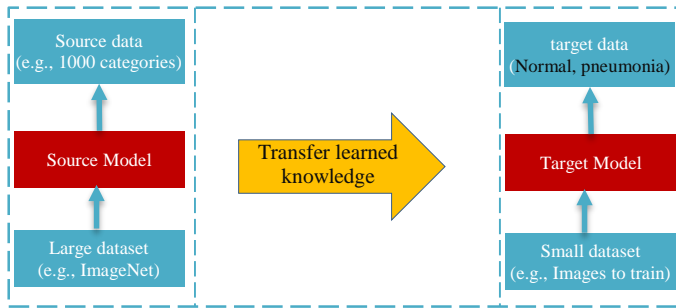


Fig. 5. Transfer Learning Behavior.

H. Model Architecture

Four models were trained with the normal and pneumonia images used in this work. The following is a detailed description of the models presented in this work.

1) *VGG16*: VGG16 is a CNN model that achieved 92.7% accuracy among the top five in the ImageNet dataset containing more than 14 million images divided into 1000 categories [22]. The main reasons for using this model are a) its architecture is easy to understand as well as its implementation; b) it contains relatively few convolutional layers: 13 convolutional and 3 dense layers; c) it has been trained with the ImageNet database.

This model starts with an input image of dimensions (224,224,3), as shown in Fig. 6. The first two layers are composed of 64 channels with a filter size of (3,3), then, after a layer (2,2), there are two convolutional layers with 256 channels and with a filter size of (3,3). After that, there are two sets of three convolution layers and a maximum group layer, with 512 channels and filter size (3,3). And so on, successively, until the dense layers are reached.

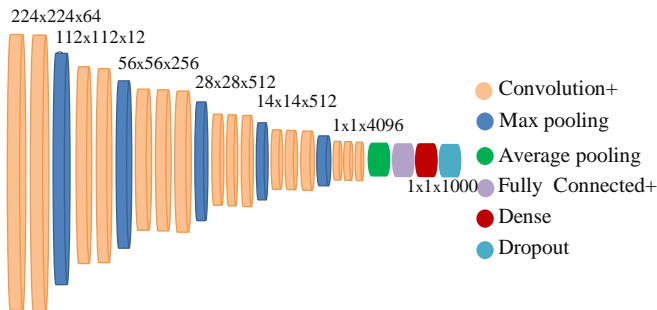


Fig. 6. Architecture of VGG16.

2) *VGG19*: The VGG19 model is very similar to VGG16, they follow the same logic, with the difference that VGG19 has a greater number of layers, but the objective of both models is common: to filter the image keeping only the discriminant information. The VGG19 model has five blocks as shown in Table I. The first two contain two convolutional layers with filter sizes of 64 and 128; the middle block contains four convolutional layers with a filter size of 256, and the last two contain two convolutional layers with a filter size of 512 each [23].

This model, in its first phase, freezes the entire network, except for the fully connected layer. In a very similar way, as in the VGG16 model, the same connected layer has been used in the VGG19 model. Then, in the second layer, the last four convolutional layers are unfrozen to learn new features. The architecture of the model is shown in Table I.

TABLE I. VGG19 MODEL ARCHITECTURE

Type	N° Filters / Parameters			
2 Conv2D	64	64		
Max Pool	N/A			
2 Conv2D	128	128		
Max Pool	N/A			
4 Conv2D	256	256	256	256
Max Pool	N/A			
4 Conv2D	512	512	512	512
Max Pool	N/A			
4 Conv2D	512	512	512	512
Max Pool	N/A			
3 layers Fully-Connect	4096	4096	1000	
Softmax	N			

3) *ResNet50*: ResNet is classified in the residual networks category. It was developed by Microsoft Research and managed to win first place in the IRSVRC 2015 competition, obtaining a 3.57% margin of error in the top five [12]. It is mainly used for image classification. In this type of network, instead of waiting for the layers to conform to the desired mapping, it is left to conform to a residual mapping. Residual learning is adopted for every certain number of stacked layers. Formally, a building block described in equation 1.1 is considered.

$$y = F(x, w_i) + x \tag{1.1}$$

Where x is the input y , y is the output of the considered layer group, and $F(X, W_i)$ represents the residual mapping to be learned. There are two types of blocks for residual networks [24]. The building block is composed of two convolutional layers with a 3x3 size filter; and the bottleneck building block is composed of three convolutional layers, the first and third layers with 1x1 filters, the second with a 3x3 filter as can be seen in Fig. 7.

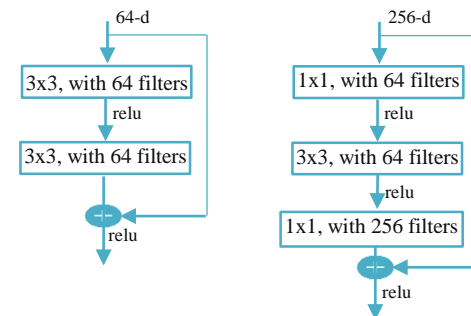


Fig. 7. Representation of the Building Block and the Bottleneck Building Block.

4) *Inception-v3*: Inception -v3, is a deep CNN with 42 layers, developed by Google, has a high image classification performance, and is integrated by: convolution layers, avg Pool, MaxPool, Concat, DropOut, Fully Connected and softmax, as shown in Fig. 8. The network has multiple versions from Inception -v1, Inception -v2 and Inception -v4, each version has been presenting significant improvements for

a better adaptation of the model [25]. This version is much more complex to train; it takes more time, even days. However, this problem is solved with TL [26], since the last layer of the model is preserved for the new classes and, the Inception-v3 model is undone by removing the last layer through the TL technique.

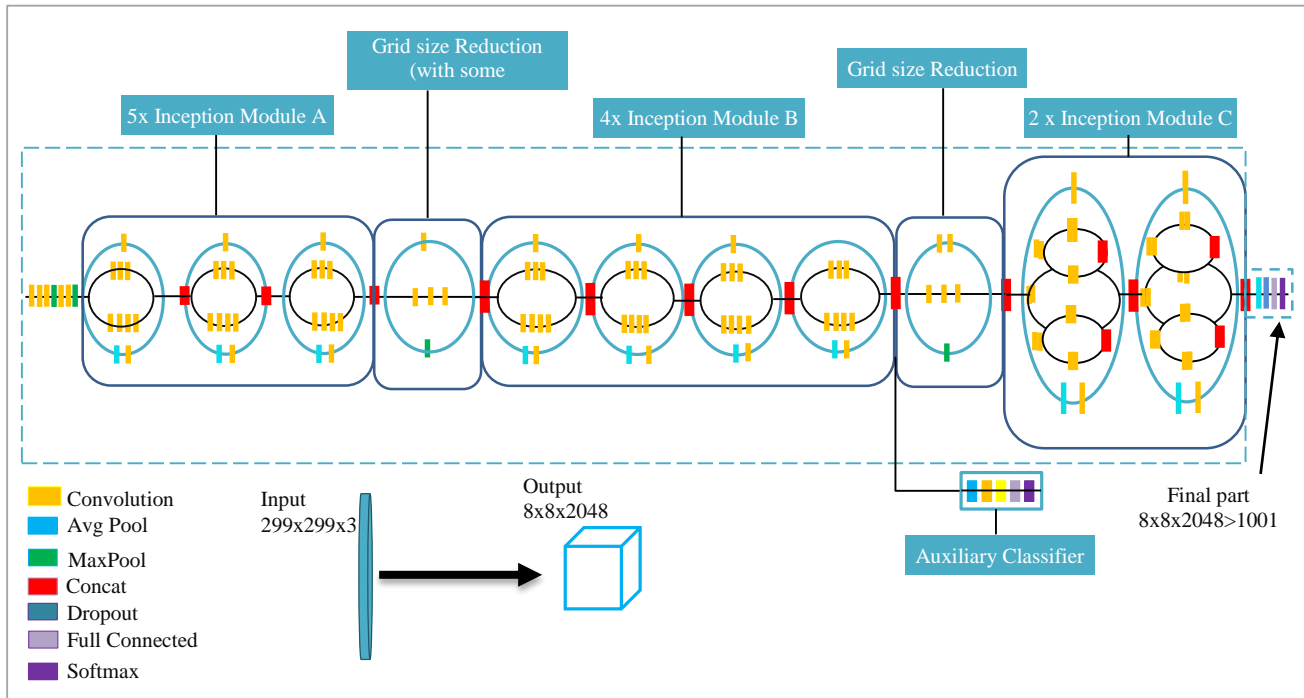


Fig. 8. Architecture of Inception-v3.

IV. RESULTS AND DISCUSSIONS

This section presents the results of the four models trained and validated with a dataset of 5840 chest X-ray images with pneumonia and, is organized as follows: 5216 chest X-ray images for training and 624 images for model validation. The same processing technique, the same amount of data, and the same number of partitions were used for all four models. With the predicted values, the confusion matrix was constructed for all models, where the predictions are synthesized and compared with the real values. For example, Fig. 9 shows the confusion matrix of the VGG19 model, where the true positives (correct positive predictions), true negatives (correct negative predictions), false positives (incorrect positive prediction), and false negatives (incorrect negative prediction) can be observed.

Similarly, to measure the performance of each of the models, the Accuracy function was used to evaluate the overall correct predictions (true positives and true negatives) among the total predictions (true positives, false positives, true negatives and false negatives). Loss, this function calculates the incorrectly classified predictions (false positives and false negatives), among the total predictions (true positives, false positives, true negatives, and false negatives). This gives us a clearer picture of how well the model is performing. Recall allows us to determine how many of the predicted positives were found to be correct.

The recall or sensitivity to measure the quality of a machine learning model is extremely important in classification tasks. Recall, which is responsible for calculating the percentage of hits, is also known as sensitivity. F1-Score allows the combining of both Accuracy and Recall into a single weighted measure. If the F1-Score is high, this means that false positives and false negatives are low.

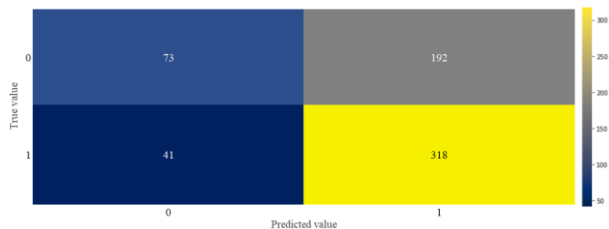


Fig. 9. Confusion Matrix of the VGG19 Model.

Graphs were also constructed to evaluate the performance of each of the models as the epochs developed. As shown in Fig. 10, 11, 12, and 13, the performance of the models presented in this work is analyzed below.

Fig. 10, 11, 12, and 13 show a comparison between Accuracy and loss, i.e. the error with training and validation data. The error with the training data is much smaller as we increase the number of epochs. In contrast, in the validation data, Loss differs a lot from its real value as the number of epochs increases, thus it is very unstable. Regarding the accuracy, the blue line indicates that the accuracy percentage of the model is very close to one as the number of epochs increases, unlike the accuracy in the validation data, where it is very high for some cases.

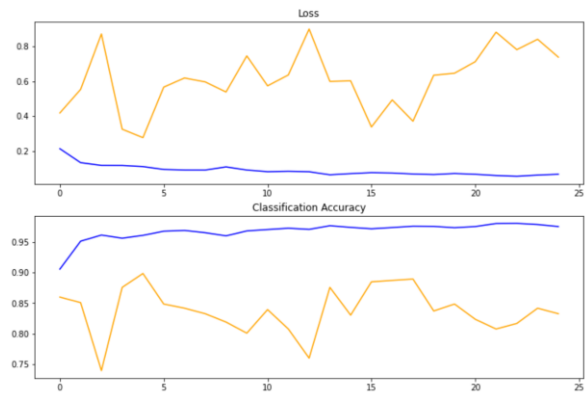


Fig. 10. Accuracy and Data Loss of the VGG16 Model.

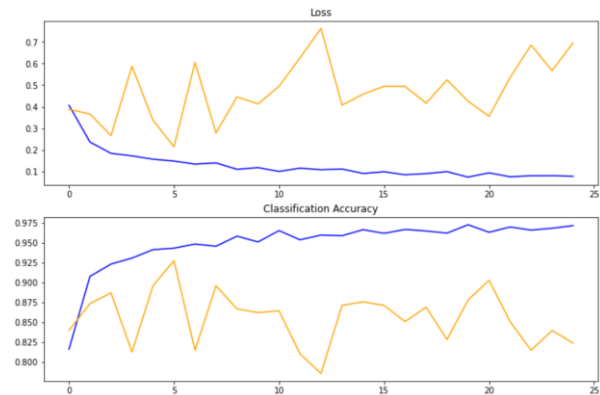


Fig. 11. Accuracy and Data Loss of the VGG19 Model.

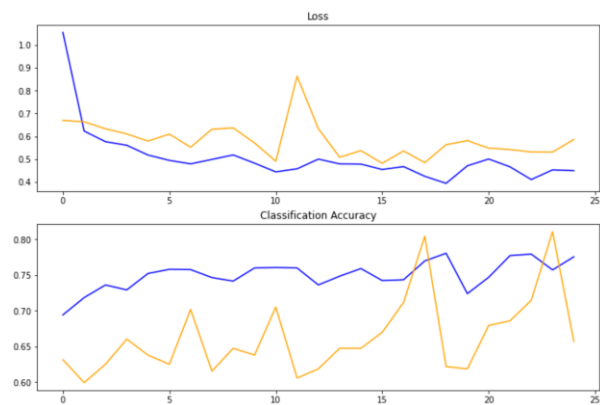


Fig. 12. Accuracy and Data Loss of the ResNet50 Model.

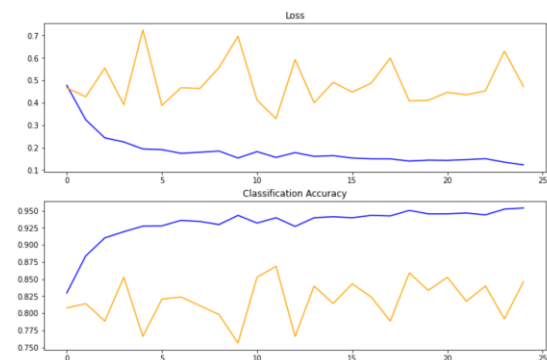


Fig. 13. Accuracy and Loss of Data from Inception-v3.

In the evaluation of the results, the two types of patients were taken into account: normal patients and patients with pneumonia. The confusion matrix in Table II shows the error generated by each model. This helps us to know the performance of each model in the classification of the validation images. Table II shows the confusion matrix of the four CNN models.

TABLE II. CONFUSION MATRIX OF THE MODELS UNDER STUDY

Model	Predicted	
VGG19	71	194
	40	319
VGG19	73	189
	41	321
ResNet50	63	178
	18	365
Inception-v3	86	144
	25	369

Concerning the performance values for each model, the recall and F1-Score are calculated based on the above-described confusion matrices. A comparison of the training and data validation results for each model is presented below.

With the results in Tables III and IV, it is resolved that the VGG16 model in training managed to obtain an accuracy of 62.5% and a loss of 41%, respectively. Similarly, for the VGG19 model, the level of accuracy in training shows a slight improvement, reaching 63.1% and a 41% loss in validation. With the ResNet50 model, the training accuracy shows a significant improvement, reaching 68.6% accuracy, and a 37% loss in validation. Finally, the InceptionV3 model evidences a better performance, achieving 72.9% accuracy in training and a 23% loss in validation. Therefore, it can be concluded that the InceptionV3 model has outperformed the VGG16, VGG19, and ResNet50 models, given that it has achieved the best values in each performance measure, both in accuracy and F1-score, demonstrating that it is a coherent and effective model obtaining a score of over 93% in the recall, although ResNet50 also obtained an excellent recall score of 95.3%. Inceptionv3 is superior in accuracy with 72.9% and F1-Score with 82%. Models VGG16, VGG19, and ResNet50 did not achieve the best score, as can be seen in Fig. 10, 11, and 12, which show the accuracy and loss value of each model.

TABLE III. VALUES OF MODEL PERFORMANCE MEASURES

Model	Accuracy	Recall	F1
VGG16	62.5%	88.9%	73.4%
VGG19	63.1%	88.7%	73.8%
ResNet50	68.6%	95.3%	79.8%
InceptionV3	72.9%	93.7%	82%

TABLE IV. PRECISION AND LOSS VALUES FOR EACH MODEL

Model	Training		Validation	
	Accuracy	loss	Accuracy	Loss
VGG16	70%	31%	62.5%	41%
VGG19	72%	32%	63.1%	39%
ResNet50	69%	36%	68.6%	37%
InceptionV3	83%	24%	72.9%	23%

In the TL models, the confusion matrices represent the margin of error in the classifier models. The results obtained from the training and validation data are shown in Table IV. Note that models VGG16, VGG19, and ResNet50 show relatively high overfitting concerning InceptionV3 because the difference between the accuracy obtained in the training and the accuracy obtained with the validation data is very noticeable. These three models have high losses and their accuracy is also low, therefore, these three models have poor performance, and little efficiency could be improved or trained with more data volume. In general, the VGG19 model performs better than the VGG16 model; the ResNet50 model outperforms the VGG16 and VGG19 models in all metrics (accuracy, recall, and F1-score), respectively. The accuracy obtained in the training and the loss value can be seen in Fig. 10, 11, and 12, where the variations of the accuracies are shown according to the number of epochs that are increased. The models used in this work correspond to deep CNNs, each model with a certain number of layers. Their accuracy can improve with a higher volume of data for training.

V. CONCLUSION

This paper presents four high-performance CNN models for application in real medical cases. All four models have high training accuracy rates. Recall is an important factor in measuring performance since it is important to reduce the number of false negatives in the image processing to be trained. While the ResNet50 model achieved the best recall of 95.3%, the Inceptionv3 model also achieved a recall of 93.7%, and the two models with the best F1-Score of 79.8% and 82% respectively.

The Inceptionv3 model is the best performing model in terms of accuracy and F1 score; therefore, it is the model that achieved the highest training efficiency. This model can be used by clinicians to detect pneumonia early in both children and adults. This model can be taken to an automated process to process a large number of X-ray images automatically and provide accurate diagnostic results, helping healthcare facilities to provide better patient services and thus reduce the mortality rate from this disease.

For future work, they seek to improve the accuracy of the models with new tuning parameters and optimizers. In [27] they presented a model based on Xception for the detection of breast cancer in real-time. The InceptionV3 model, which is the best performing model in this work, can be extended to classify other diseases as [27] has done with good results. The performance of the models can be improved with a larger amount of data.

ACKNOWLEDGMENT

To the PhD program of the Escuela Técnica Superior de Ingenieros de Telecomunicación, Universidad Politécnica de Madrid, Spain.

REFERENCES

- [1] Organización Mundial de la Salud, “Neumonía,” 2021. <https://www.who.int/es> (accessed Aug. 24, 2022).
- [2] R. Kundu, R. Das, Z. W. Geem, G. T. Han, and R. Sarkar, “Pneumonia detection in chest X-ray images using an ensemble of deep learning models,” *PLoS One*, vol. 16, no. 9 September, Sep. 2021, doi: 10.1371/JOURNAL.PONE.0256630.
- [3] M. I. Neuman *et al.*, “Variability in the interpretation of chest radiographs for the diagnosis of pneumonia in children,” *J Hosp Med*, vol. 7, no. 4, pp. 294–298, Apr. 2012, doi: 10.1002/JHM.955.
- [4] G. J. Williams *et al.*, “Variability and accuracy in interpretation of consolidation on chest radiography for diagnosing pneumonia in children under 5 years of age,” *Pediatr Pulmonol*, vol. 48, no. 12, pp. 1195–1200, Dec. 2013, doi: 10.1002/PPUL.22806.
- [5] V. Sirish Kaushik, A. Nayyar, G. Kataria, and R. Jain, “Pneumonia Detection Using Convolutional Neural Networks (CNNs),” in *Lecture Notes in Networks and Systems*, vol. 121, Springer, 2020, pp. 471–483. doi: 10.1007/978-981-15-3369-3_36.
- [6] A. Fourcade and R. H. Khonsari, “Deep learning in medical image analysis: A third eye for doctors,” *J Stomatol Oral Maxillofac Surg*, vol. 120, no. 4, pp. 279–288, Sep. 2019, doi: 10.1016/J.JORMAS.2019.06.002.
- [7] O. Iparraguirre-Villanueva, V. Guevara-Ponce, F. Sierra-Liñan, S. Beltozar-Clemente, and M. Cabanillas-Carbonell, “Sentiment Analysis of Tweets using Unsupervised Learning Techniques and the K-Means Algorithm,” *International Journal of Advanced Computer Science and Applications*, vol. 13, no. 6, pp. 571–578, 2022, doi: 10.14569/IJACSA.2022.0130669.
- [8] T. Rahman *et al.*, “Transfer Learning with Deep Convolutional Neural Network (CNN) for Pneumonia Detection Using Chest X-ray,” *Applied Sciences 2020, Vol. 10, Page 3233*, vol. 10, no. 9, p. 3233, May 2020, doi: 10.3390/AP10093233.
- [9] P. Chhikara, P. Singh, P. Gupta, and T. Bhatia, “Deep convolutional neural network with transfer learning for detecting pneumonia on chest x-rays,” *Advances in Intelligent Systems and Computing*, vol. 1064, pp. 155–168, 2020, doi: 10.1007/978-981-15-0339-9_13/COVER.
- [10] G. Labhane, R. Pansare, S. Maheshwari, R. Tiwari, and A. Shukla, “Detection of Pediatric Pneumonia from Chest X-Ray Images using CNN and Transfer Learning,” *Proceedings of 3rd International Conference on Emerging Technologies in Computer Engineering: Machine Learning and Internet of Things, ICETCE 2020*, pp. 85–92, Feb. 2020, doi: 10.1109/ICETCE48199.2020.9091755.
- [11] M. Salehi, R. Mohammadi, H. Ghaffari, N. Sadighi, and R. Reiazi, “Automated detection of pneumonia cases using deep transfer learning with paediatric chest X-ray images,” *British Journal of Radiology*, vol. 94, no. 1121, May 2021, doi: 10.1259/BJR.20201263.
- [12] R. Jain, P. Nagrath, G. Kataria, V. Sirish Kaushik, and D. Jude Hemanth, “Pneumonia detection in chest X-ray images using convolutional neural networks and transfer learning,” *Measurement (Lond)*, vol. 165, Dec. 2020, doi: 10.1016/j.measurement.2020.108046.
- [13] G. Liang and L. Zheng, “A transfer learning method with deep residual network for pediatric pneumonia diagnosis,” *Comput Methods Programs Biomed*, vol. 187, p. 104964, Apr. 2020, doi: 10.1016/J.CMPB.2019.06.023.
- [14] M. M. Tareh, N. Zhu, T. A. A. Ali, A. S. Hameed, and M. L. Mutar, “Transfer Learning to Detect COVID-19 Automatically from X-Ray Images Using Convolutional Neural Networks,” *Int J Biomed Imaging*, vol. 2021, 2021, doi: 10.1155/2021/8828404.
- [15] I. D. Apostolopoulos and T. A. Mpesiana, “Covid-19: automatic detection from X-ray images utilizing transfer learning with convolutional neural networks,” *Phys Eng Sci Med*, vol. 43, no. 2, pp. 635–640, Jun. 2020, doi: 10.1007/S13246-020-00865-4/TABLES/6.
- [16] O. Dahmane, M. Khelifi, M. Beladgham, and I. Kadri, “Pneumonia detection based on transfer learning and a combination of VGG19 and a CNN built from scratch,” *Indonesian Journal of Electrical Engineering and Computer Science*, vol. 24, no. 3, pp. 1469–1480, Dec. 2021, doi: 10.11591/IJEECS.V24.I3.PP1469-1480.
- [17] J. Rubin Jonathan, D. Sanghavi, C. Zhao, K. Lee KathyLee, A. Qadir, and M. Xu-Wilson, “Large Scale Automated Reading of Frontal and Lateral Chest X-Rays using Dual Convolutional Neural Networks,” Apr. 2018, doi: 10.48550/arkiv.1804.07839.
- [18] Y. Xu, Z. Jia, Y. Ai, F. Zhang, M. Lai, and E. I. C. Chang, “Deep convolutional activation features for large scale Brain Tumor histopathology image classification and segmentation,” *ICASSP, IEEE International Conference on Acoustics, Speech and Signal Processing - Proceedings*, vol. 2015-August, pp. 947–951, Aug. 2015, doi: 10.1109/ICASSP.2015.7178109.
- [19] A. Jain, S. Ratnoo, and D. Kumar, “Convolutional neural network for Covid-19 detection from X-ray images,” *Proceedings - 2021 4th International Conference on Computational Intelligence and Communication Technologies, CCICT 2021*, pp. 100–104, Jul. 2021, doi: 10.1109/CCICT53244.2021.00030.
- [20] G. E. Hinton, N. Srivastava, A. Krizhevsky, I. Sutskever, and R. R. Salakhutdinov, “Improving neural networks by preventing co-adaptation of feature detectors,” Jul. 2012, doi: 10.48550/arkiv.1207.0580.
- [21] T. Mehta and N. Mehendale, “Classification of X-ray images into COVID-19, pneumonia, and TB using cGAN and fine-tuned deep transfer learning models,” 2021, doi: 10.1007/s42600-021-00174-z.
- [22] J. C. Valero Gómez, A. P. Zúñiga Incalla, and J. C. Clares Perca, “Algoritmos de Deep Learning para la detección de Neumonía en infantes a través de imágenes de radiografías del tórax,” in *Actas del Congreso Internacional de Ingeniería de Sistemas*, 2021, pp. 183–194. doi: 10.26439/ciis2021.5586.
- [23] Z. E. M. C. O. C. L. G. B. G. I. F. V.-L. A. Y. R. Eduardo Díaz Gaxiola, “Estudio comparativo de arquitecturas de CNNs en hojas de Pimiento Morron infectadas con virus”.
- [24] J. C. Valero Gómez, A. P. Zúñiga Incalla, and J. C. Clares Perca, “Algoritmos de Deep Learning para la detección de Neumonía en infantes a través de imágenes de radiografías del tórax,” in *Actas del Congreso Internacional de Ingeniería de Sistemas*, 2021, pp. 183–194. doi: 10.26439/ciis2021.5586.
- [25] J. S. Kumar, S. Anuar, and N. H. Hassan, “Transfer Learning based Performance Comparison of the Pre-Trained Deep Neural Networks,” *International Journal of Advanced Computer Science and Applications*, vol. 13, no. 1, pp. 797–805, 2022, doi: 10.14569/IJACSA.2022.0130193.
- [26] M. Mujahid *et al.*, “Pneumonia Classification from X-ray Images with Inception-V3 and Convolutional Neural Network,” 2022, doi: 10.3390/diagnostics12051280.
- [27] B. S. Abunasser, M. R. J. AL-Hiealy, I. S. Zaqout, and S. S. Abu-Naser, “Breast Cancer Detection and Classification using Deep Learning Xception Algorithm,” *International Journal of Advanced Computer Science and Applications*, vol. 13, no. 7, 2022, doi: 10.14569/IJACSA.2022.0130729.